Unveiling the Role of Base and Additive in the Ullmann-type of Arene-Aryl C-C Coupling Reaction

Ajitha J. Manjaly,[a] Fathima Pary,[b] Toby L. Nelson[b,*], and Djamaladdin G. Musaev[a,*]

[a] Cherry L. Emerson Center for Scientific Computation, and Department of Chemistry, Emory University, 1515 Dickey Drive, Atlanta, Georgia 30322

[b] Department of Chemistry, Oklahoma State University, 107 Physical Science, Stillwater, Oklahoma 74078

Supporting Information Placeholder

ABSTRACT: The mechanism of Ullmann-type biaryl formation between benzo-[1,2-*b*:4,5-*b'*]dithiophene-1,1,5,5-tetraoxide (BDTT) and iodobenzene (ArI) was computationally studied in the presence of CuI, phenanthroline (Phen), K_3PO_4 (as a base) and Ag_2CO_3 (as an additive). It is also shown that base and additive play critical roles in each steps of the reaction, such as: (a) the *I-to-base exchange* in complex (Phen)CuI, (b) substrate deprotonation via the *acid-base mechanism*, and (c) Ar–I activation and DBT–Ar coupling. It is shown that: (a) the presence of sulfonyl oxygens in DBT is essential – it plays an anchoring role and brings substrate and base closer to each other. In the presence of K_3PO_4 and in the absence of additive Ag_2CO_3, the Ph-I activation and C-C coupling, *occurs via a Cu-mediated nucleophilic substitution mechanism*, and requires a significant free energy barrier. However, the addition of Ag_2CO_3 to the reaction mixture, not only accelerates the DBT and PhI coupling by reducing the rate-limiting Ph-I activation barrier, but also switches the mechanism of the reaction from a *Cu-mediated nucleophilic substitution* to a *Ag(I)-promoted oxidative addition-reductive elimination.* The findings are important for development of the next generation reaction conditions for Ullmann-type of coupling reactions.

INTRODUCTION

Arenes and heteroarenes are commonly used compounds in the synthesis of pharmaceuticals and in the design of organic electronic devices such as organic light emitting diodes (OLEDs), photovoltaics, transistors and batteries.[1-4] Utilization of these aromatic species involves selective functionalization of their C(sp^2)–H bonds. Currently, several synthetic methodologies have been established for the functionalization of arene C(sp^2)–H bonds[5-10] including Ullmann-type catalytic arene arylation and amination reactions.[11-15] Recently, Nelson and coworkers have applied this strategy to the copper catalyzed direct C-H arylation of benzo-[1,2-*b*:4,5-*b'*]dithiophene-1,1,5,5-tetraoxide (BDTT) with aryl iodides (Scheme 1).[16] This new reaction opens a way for the efficient utilization of electron poor heterocycles in organic semiconductor design. In this work, the authors coupled BDTT as a nucleophile with (hetero)aryl iodides as electrophiles in the presence of CuI and 1,10-phenanthroline (Phen) ligand as a catalyst, K_3PO_4 as a base, and Ag_2CO_3 as an additive.

However, a lack of in-depth understanding of mechanistic details, role of catalyst, ligand, base, additive, nucleophile and electrophile in this reaction limits its broader application. In order to overcome these shortcomings, more comprehensive studies elucidating the intimate mechanistic details of this reaction, and identifying the role of the reaction components are necessary.

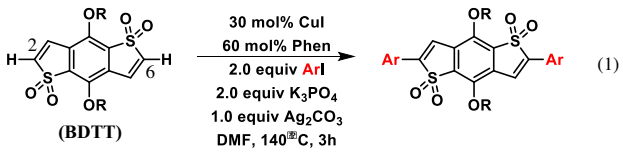

(1)

Scheme 1. Copper catalyzed C-H direct arylation of benzo-[1,2-*b*:4,5-*b'*]dithiophene-1,1,5,5-tetraoxide (BDTT) with aryl iodides [17].

In general, the mechanism of the Ullmann-type couplings has long been a subject of numerous experimental and computational studies but remains a topic of active debates.[17-23] It is established that the mechanism of these reactions strongly depend not only on the nature of the Cu(I)-complex and ancillary ligand (phenanthrolines,[24-25] bipyridines,[26] diamines,[27-29] dipyridylimines,[30] amino acids,[31] 8-

hydroxyquinolines,[32] diketones,[33-34] pyridylketones,[35] and others), but also on the nature of electrophile, nucleophile, base and additive. In the case of widely used neutral and bidentate ancillary ligands (LL) such as phenanthrolines, bipyridines, and diamines,[36-40] an oxidative addition/reductive elimination (OA/RE) mechanism (Scheme 2a) that starts from the three-coordinated intermediate, (LL)Cu(Nu), was proposed. A radical mechanism for the reaction of haloarenes with (LL)Cu(Nu) has been proposed earlier[17] but have been discounted because of invalidating negative radical clock experiments and lack of inhibition by radical scavengers.[41-44]

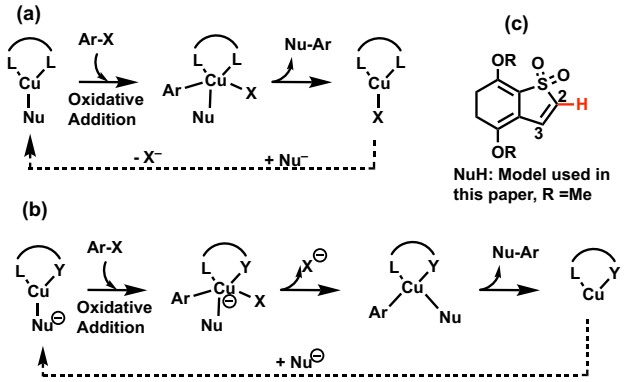

Scheme 2. Previously proposed mechanisms of the Ullmann-type Cu(I)-catalyzed C-C coupling with (a) neutral (LL) and (b) anionic (LY) ancillary ligands (also, see [22]). Here, (c) is a model nucleophile, 4,7-dimethoxybenzo[*b*]thiophene 1,1-dioxide (DBT), used in the present study.

Similarly, the Ullmann biaryl ether formation catalyzed by Cu(I) in the presence of anionic bidentate ancillary ligands [H(LY)], such as 8-hydroxyquinolines[32] and diketones,[33-34] is proposed (see Scheme 2b) to start from the reactive three-coordinated anionic intermediate $[(LY)Cu(Nu)]^-$: in the case of Nu = OPh, this intermediate reacts with the iodoarene to form five-coordinated, $[(Ar)(I)Cu(LY)(PhO)]^-$, Cu(III) complex, which later releases iodide anion and proceeds via the Ar-Nu bond formation and re-generation of the Cu(I)-catalyst.[22] Based on the available experimental data, the oxidative addition of an iodoarene is proposed to be the rate-determining step of the reaction.[22] It is necessary to emphasize that, this "*modified anionic mechanism*", proposed by Hartwig and coworkers for the reaction of iodobenzene with phenoxides,[22] is different from that reported for the reaction of iodobenzene with the alcohol and amine (of 5-aminopentanol) in the presence of a similar anionic ligand.[17-18] The difference between the mechanisms of the reactions of phenoxides and those of alcohols and amines was rationalized by the greater stability of anionic aryloxide-containing complexes $[(LY)Cu(OAr)]^-$ than its anionic alkoxide counterparts.

However, previous extensive mechanistic studies, have generally left unanswered the roles of base and additive both in the formation of three-coordinated $[(LL)Cu(Nu)]$ and $[(LY)Cu(Nu)]^-$ intermediates, and in the following aryl-halide bond activation and Nu-Ar coupling steps. Available experiments on the Ullmann-type coupling,[45-46] including the recently reported reaction by Nelson and coworkers,[16] have unambiguously demonstrated importance of the base and additive. It is conceivable that these metal salts not only act as oxidants during the catalyst regeneration but also assist other steps of the catalytic cycle.[23, 47] Recent report of Gurjar and Sharma[48] have indicated that the CO_3^{2-}/PO_4^{3-} anion may act as a chelating ligand in the Cu(I)-catalyzed C-N coupling and facilitate the reductive elimination from the Cu(III)-intermediate. However, the reported reaction mechanism and characterized Cu(III) species are not directly applicable and illustrative for the Ullmann-type catalytic reactions in the presence of base and additive because they were performed under sequential addition of aryl iodide and carbonate base. For example, the following reaction sequence illustrates several possible steps:

$\{[(LL)Cu^{I}(HNNu)]^+ + PhI \rightarrow [(LL)Cu^{III}(HNNu)(Ph)(I)]^+$ then $[(LL)Cu^{III}(HNNu)(Ph)(I)]^+ + CO_3^{2-} \rightarrow [(LL)Cu^{III}(HNNu)(Ph)(CO_2)]\}$.

Furthermore, as emphasized previously, the nature of the nucleophile is also crucial in the Ullmann-type of coupling.[17, 20] As such, the BDTT reagent used in the reaction presented in Scheme 1 was not previously explored in mechanistic studies, and possesses sulfonyl oxygens, the role of which remains elusive in the studied C–C coupling reaction.

In order to answer these questions, herein, we investigate the mechanisms of CuI and phenanthroline (Phen) catalyzed, and K_3PO_4 and Ag_2CO_3 facilitated biaryl formation between BDTT and aryl iodides. We expect that the acquired knowledge from the proposed research will (a) enhance the development of next generation reaction conditions for utilization of electron poor heterocycles, such as BDTT, in organic semi-conductor design, and (b) help delineate some of the remaining mechanistic issues for Ullmann-type of couplings.

Herein, we show that base and additive play critical roles in each steps of the reaction, such as (a) the *I*-

to-base exchange in complex (Phen)CuI, (b) substrate deprotonation via the *acid-base mechanism*, and (c) Ar–I activation and DBT–Ar coupling. The presence of sulfonyl oxygens in DBT is also essential, and plays an anchoring role. We demonstrated that, in the presence of K_3PO_4, the reaction proceeds *via a Cu-mediated nucleophilic substitution mechanism*, and requires significant free energy barrier. However, addition of Ag_2CO_3 to reaction mixture not only reduces the rate-limiting Ar–I activation barrier, but also switches mechanism of the reaction from the *Cu-mediated nucleophilic substitution* to the *oxidative addition/reductive elimination occurring on the Ag^+-cation of the additive.* Thus, the Ag-center of additive Ag_2CO_3 acts as a catalytic active center and undergoes an Ag(I)/Ag(III) oxidation.

METHODS

Computational Details. The presented calculations were carried out using the Gaussian 09 suite of programs.[49] Geometry of all reported reactants, intermediates, transition states (TSs) and products were optimized without symmetry constraint at the B3LYP level of density functional theory (DFT)[50-51] in conjunction with Lanl2dz basis set and corresponding Hay-Wadt effective core potential (ECP) for Cu, Ag and I atoms.[52-53] Standard 6-31G(d,p) basis sets were used for all remaining atoms. Dispersion corrections were included into the calculation at the Grimme's DFT-D3 level of theory.[54] Below, this approach will be designated as [B3LYP-D3]/{Lanl2dz+[6-31G(d,p)]}. Bulk solvent effects are incorporated into calculations at the self-consistent reaction field polarizable continuum model (IEF-PCM) level[55-56] by selecting DMF as the solvent (eps=36.71, rsolv=2.647, density=0.00778, epsinf=1.75).[57] The nature of each stationary point was characterized by the presence of zero or one imaginary frequencies for minima and TSs, respectively. The IRC calculations were performed to confirm nature of each TSs. The relative enthalpies (ΔH) and Gibbs energies (ΔG) are presented as ΔH/ΔG, and calculated under standard conditions (1 atm and 298.15 K). Cartesian coordinates of all reported structures are given in the Supporting Information.

Here, for practical reasons, in the presented computational studies, we modelled BDTT by 4,7-dimethoxybenzo[*b*]thiophene 1,1-dioxide (DBT) (see Scheme 2c).

Results and Discussion

A. Catalyst Activation: In the presence of PhI and base in the reaction mixture, the studied reaction will be initiated by interaction of (Phen)CuI (**1**) with either available base/additive (K_3PO_4/Ag_2CO_3) or electrophile PhI. Computations show that the PhI interaction with **1** is thermodynamically less favorable than with K_3PO_4 and Ag_2CO_3 (see Figure S1 of supporting materials). Meantime, the interaction of (Phen)CuI (**1**) with K_3PO_4, which is exergonic by -30.2/-17.2 kcal/mol, initiates the iodide removal with only a 0.0/2.1 kcal/mol free energy barrier at the transition state **TS1a** (the $\Delta E^{\ddagger}$ value is 0.3 kcal/mol) (see Figure 1). Interestingly, at the current level of theory, in the product **3a** the formed KI fragment stays coordinated to the PO_4-unit of K_3PO_4: the calculated (Phen)Cu(K_2PO_4)–(KI) bonding free energy is 10.7 kcal/mol.

Briefly, the interaction of (Phen)CuI with Ag_2CO_3 is found to be stronger (the calculated [(Phen)CuI]–[Ag_2CO_3], (**2b**), bonding energy is -34.3/-21.5 kcal/mol) than with K_3PO_4, iodide removal from **2b** occurs with almost no energy barrier ($\Delta G^{\ddagger}$ = 0.4 kcal/mol), and the overall reaction leads to the formation of (Phen)Cu[$AgCO_3$(AgI)] intermediate (**3b**) is more exergonic (by -40.1/-27.7 kcal/mol, see Figure S2 of Supporting materials).

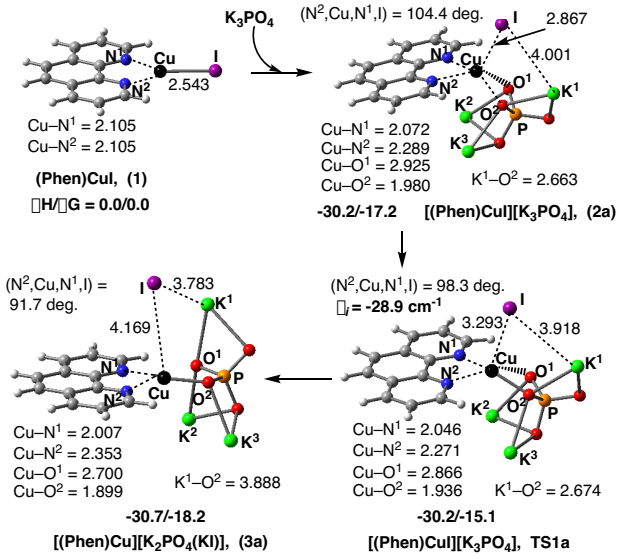

Figure 1. Reactants, intermediate, transition state and product of the reaction of (Phen)CuI with K_3PO_4, along with their relative energies (in kcal/mol) and important geometry parameters (distances in Å and angles in degree). The calculated ΔE values of structures **2a, TS1a** and **3a** are -31.1, -30.8 and -32.0 kcal/mol, respectively.

At the next stage, in the presence of substrate (DBT) and PhI, intermediate **3a** (or **3b**) may participate in two competing processes. One of them, called as "*the Ar–I activation first*", starts by the ArI coordination

and proceeds via the Ar–I bond activation. Then, the resulting complex coordinates DBT nucleophile, activates its C–H bond, and leads to the C–C coupling product. Calculations show that this process requires high energy barriers (see Figures S3a and S3b of Supporting Materials) and cannot compete with the alternative, "*the substrate C–H activation first*", pathway.

B. Mechanism of the "Substrate C-H activation first" pathway: This pathway of the reaction starts by the substrate (DBT) coordination to complex **3a** and formation of the adduct [(Phen)Cu][K_2PO_4(KI)](DBT), **4a**, with -20.9/-4.3 kcal/mol free energy. As shown in Figure 2, one of the stabilizing factors in the resulting complex **4a** is an interaction between one of the sulfonyl oxygens (namely, O^3-center) of DBT and the cation K^2 of the coordinated $[K_2PO_4(KI)]^-$ ligand. Other stabilizing factors could involve the interaction of Cu with C^1, hydrogen bonding between the substrate C^1–H^1 bond and O^1-center of base, and π-π interaction between the phenanthroline ligand and aromatic ring of the DBT substrate.

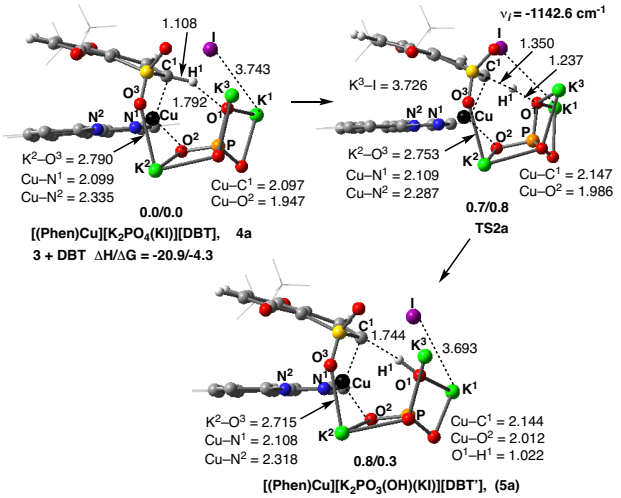

Figure 2. Pre-reaction complex **4a**, substrate C-H activation transition state **TS2a** and the C-H activated product **5a**, alone with their relative energies (in kcal/mol) and important geometry parameters (distances in Å and angles in degree). The calculated ΔE values of **TS2a** and complex **5a** are 3.9 and 1.1 kcal/mol, respectively.

Thus, the presence of sulfonyl oxygens in DBT is essential for the substrate C-H bond activation: it interacts with the counter-cation of the coordinated base, brings the reactive C^1–H^1 bond of the substrate and the accepter O-center of the base closer to each other, and, consequently, facilitates the substrate C-H bond activation.

From the complex **4a,** the targeted reaction may proceed via either KI dissociation or C^1–H^1 bond activation pathways. The former process requires 14.8 kcal/mol free energy and cannot compete with the C^1–H^1 bond activation which requires only a 0.8 kcal/mol free energy barrier at the transition state **TS2a** and is almost thermoneutral.

Close analyses of **TS2a** and product complex **5a** show that the reaction **3a** + DBT → **4a** → **TS2a** → **5a** is an *acid-base process* and occurs via proton removal by the coordinated $[K_2PO_4(KI)]^-$ ligand. During this process, mainly, the C^1–H^1 bond of substrate is broken and the O^1–H^1 bond of base is formed. As shown in Figure 2, there is no evidence of either Cu–C^1 or Cu–O^2 bond formation (i.e. shortening of these bonds). Another strong support for this conclusion comes from the negative charge accumulation on the substrate during the reaction. The calculated total NBO charge of DBT' fragment (here and below DBT' stands for the deprotonated derivative of DBT) changes from 0.20 |e| to -0.12 |e| and -0.84 |e| in complex **4a**, **TS2a** and product **5a**, respectively. *Thus, the role of the transition metal center (i.e. Cu) in this step of the reaction also is to bring substrate and base closer to each other and facilitate C–H deprotonation.*

Briefly, similar results were obtained if Ag_2CO_3 was used as a base. Data presented in Supporting Materials (see Figure S4) show that substrate coordination to the complex **3b** is only 16.9/2.2 kcal/mol exergonic, which is 4.0/2.1 kcal/mol less than that obtained for K_3PO_4. However, surprisingly, deprotonation of substrate by Ag_2CO_3 requires larger free energy barrier than K_3PO_4 (11.9/12.4 kcal/mol *vs* 0.7/0.8 kcal/mol). Furthermore, product complex **5b** is highly unstable and transforms to the pre-reaction complex **4b** with almost no energy barrier. Comparison of these findings for K_3PO_4 and Ag_2CO_3 show that in the presence of both K_3PO_4 and Ag_2CO_3 in the reaction mixture, the K_3PO_4 will act as a more effective base than Ag_2CO_3.

C. Aryl-iodide Coordination: Thus, in the presence of both K_3PO_4 and Ag_2CO_3, the product of the DBT C–H bond activation is the complex [(Phen)Cu][K_2PO_3(OH)(KI)](DBT'), **5a**. In order for the reaction to proceed, this complex should coordinate aryl iodide and activate the C–I bond. Comprehensive calculations show that this step of the reaction will be initiated by substitution of K_2PO_3(OH)(KI) with either K_3PO_4 or Ag_2CO_3 before the PhI addition. This substitution-addition reaction could proceed via either stepwise (i.e. dissociative) or concerted pathways.

The stepwise mechanism includes several elementary reactions (see Scheme 3 and Figures 3 and 4).

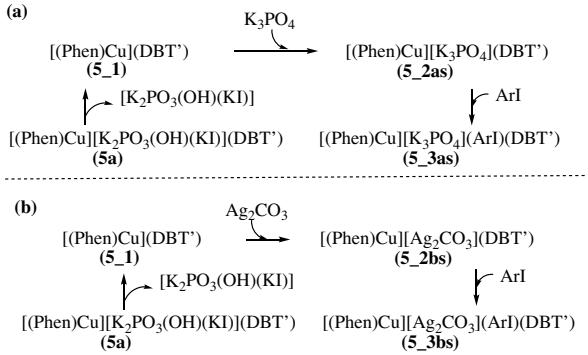

Scheme 3. Elementary reactions involved in the stepwise (a) $K_2PO_3(OH)(KI) \rightarrow K_3PO_4$ and (b) $K_2PO_3(OH)(KI) \rightarrow Ag_2CO_3$ substitution and then ArI addition.

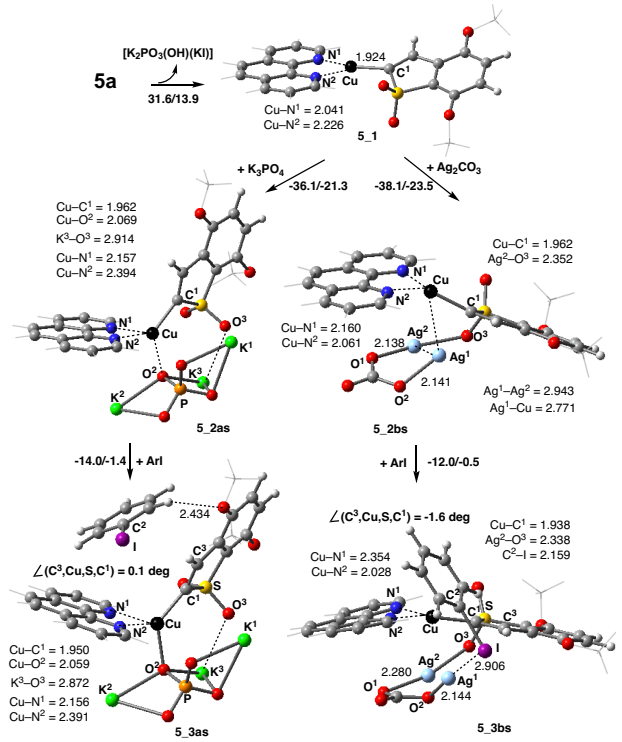

Figure 3. Intermediates **5_1**, **5_2as, 5_2bs**, **5_3as** and **5_3bs** with their important geometry parameters (distances in Å and angles in degree) of the stepwise $K_2PO_3(OH)(KI)$-to-K_3PO_4 (left) and $K_2PO_3(OH)(KI)$-to-Ag_2CO_3 (right) substitution and then ArI addition processes. Presented reaction energies (in kcal/mol) are for each specific step.

The "**s**" and "**c**" (see below) stand for the structures formed via stepwise and concerted substitution pathways, respectively.

Calculations show that the first step of the stepwise substitution processes involve the $K_2PO_3(OH)(KI)$ dissociation from **5a** to form **5_1,** requires 31.6/13.9 kcal/mol free energy (See Figure 3). However, the following step, namely, coordination of K_3PO_4 and Ag_2CO_3 to intermediate **5_1** that leads to intermediates **5_2as** and **5_2bs**, respectively, is exergonic by 21.3 and 23.5 respectively (whereas the coordination of PhI is only 2.1 kcal/mol exergonic).

*Thus, we conclude that the complexes **5_2as** and **5_2bs** are the direct analogs of the previously reported[22] three-coordinated active (LL)Cu(Nu) intermediate in the presence of K_3PO_4 and Ag_2CO_3, respectively.*

At the next step, intermediates **5_2as** and **5_2bs** coordinate aryl-iodide to form [(Phen)Cu][K_3PO_4](ArI)(DBT'), (**5_3as**) and [(Phen)Cu][Ag_2CO_3](ArI)(DBT'), (**5_3bs**) with -1.4 and -0.5 kcal/mol coordination free energies, respectively. Thus, overall, the stepwise formation of **5_3as** and **5_3bs** from **5**, PhI, K_3PO_4 and Ag_2CO_3 is exergonic by 8.8 and 10.1 kcal/mol, respectively, and occurs via 13.9 kcal/mol free energy barrier.

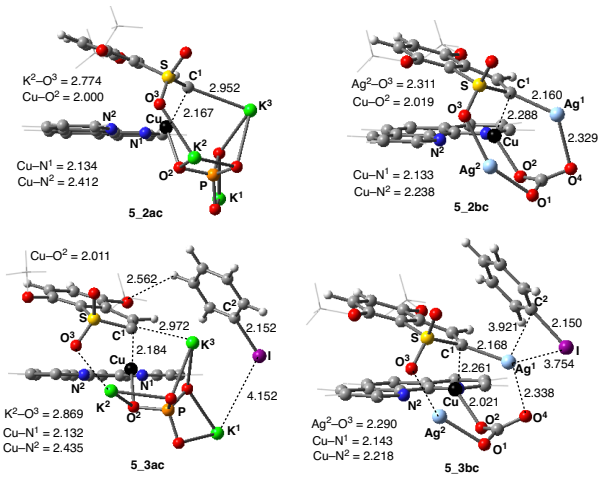

Figure 4. Intermediates **5_2ac**, **5_2bc, 5_3ac** and **5_3bc** with their important geometry parameters (distances in Å and angles in degree) of the concerted substitution of $K_2PO_3(OH)(KI)$ either by K_3PO_4 or Ag_2CO_3 in complex **5a**, respectively, and followed by the ArI addition.

We were not able to determine the transition state structures for the concerted substitution of $K_2PO_3(OH)(KI)$ either by K_3PO_4 or Ag_2CO_3. However, we have located products of these processes, complexes **5_2ac** and **5_2bc** (see Figure 4). As shown in Figure 4, in **5_2ac** and **5_2bc**, (in contrast to their **5_2as** and **5_2bs** stepwise counterparts) DBT' is only weakly coordinated to the Cu-center with the Cu-C^1 bond distances of 2.167 and 2.288 Å, respectively. However, in these complexes, the DBT' fragment, interacts with the K^+/Ag^+ cations of the base/additive via its C^1–center. In the presence of electrophile PhI, intermediates **5_2ac** and **5_2bc** react with PhI to form **5_3ac** and **5_3bc** with -2.3 and -1.7 kcal/mol coordination free energies, respectively. Calculations show that the concerted substitution reactions **5a** + PhI + K_3PO_4 → **5_3ac** +

$[K_2PO_3(OH)(KI)]$ and **5a** + PhI + Ag_2CO_3 → **5_3bc** + $[K_2PO_3(OH)(KI)]$ are exergonic by 1.2 and 16.3 kcal/mol, respectively.

At the next stage, we investigated the Ph–I bond activation and C-C coupling initiated from all of these four complexes. Inspired by the available knowledge[23, 58] and based on our comprehensive analyses, we proposed multiple mechanistic scenarios. In order to simplify our discussion, below we only present the most favorable mechanisms of the reactions, while the less favorable reaction pathways, including the single-electron transfer (SET), iodide atom transfer (IAT), various metathesis mechanisms, are given in the Supporting Materials. To make our discussion chronologically coherent, at first, we analyze mechanisms of the Ph–I bond activation and C-C coupling initiated from the complexes **5_3as** and **5_3ac** involving base K_3PO_4 and without additive Ag_2CO_3.

D. Base (i.e. K_3PO_4) assisted PhI Activation. Calculations show that in **5_3as,** the Ph–I activation occurs by as low as 34.5 kcal/mol free energy barrier via the transition state **TS3as** (see Figure 5, see also Figure S7). At this transition state iodide interacts with the K^1 cation of base, while Ar interacts with the Cu-center and, possibly, with the C^1-center of DBT'. The performed IRC calculations from **TS3as** connects pre-reaction complex **5_3as** with the C-C coupled product [(Phen)Cu][K_2PO_4(KI)(Ar-DBT')], **5_4as**. In the other words, the oxidative addition intermediate with the Cu^{III}-center is metastable and Ph-I activation at the **TS3as** leads to the C-C coupling product **5_4as**. Overall reaction **5_3as** → **TS3as** → **5_4as** is exergonic by 55.4 kcal/mol.

As mentioned previously, for K_3PO_4, the concerted substitution product **5_3ac** is less stable than stepwise one **5_3as** by ΔG = 7.6 kcal/mol. In addition, we found that it requires, about 30.9 kcal/mol of free energy barrier (i.e. 38.5 kcal/mol, relative to the **5_3as**) for the Ph-I activation at the transition state **TS3ac**. A close analysis of the geometry of **TS3ac** indicates that the Ph–I activation, similar to that in the **5_3as**, occurs simultaneously with the C–C coupling. *Thus, the Ph–I activation and C–C coupling in the complexes* **5_3as** and **5_3ac** *with K_3PO_4 can be characterized as a Cu-mediated nucleophilic substitution reactions rather than an oxidative addition-reductive elimination as it was previously reported in the base-free studies.[22] However, these reactions require large free energy barriers. 34.5 and 38.5 kcal/mol, respectively, for Ph–I bond cleavage.*

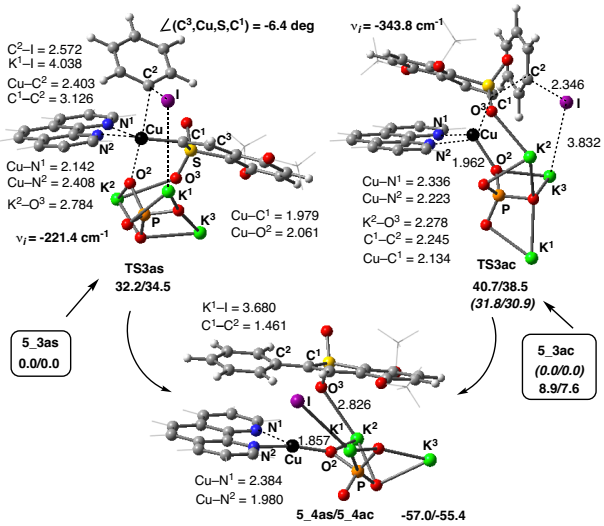

Figure 5. Transition states **TS3as** and **TS3ac**, and products **5_4as** and **5_4ac** of the Ar–I activation and C-C coupling initiated from **5_3as** and **5_3ac** with K_3PO_4 base, alone with their relative energies (calculated relative to complexes **5_3as** and **5_3ac** *(in italic)*, respectively, in kcal/mol) and important geometry parameters (distances are in Å, but angles are in deg.).

However, the available experiments show that addition of Ag_2CO_3 to the reaction mixture, as an additive, substantially increases yield of the reaction,[16] and the calculations demonstrate that the formation of the complexes **5_3bs** and **5_3bc** with Ag_2CO_3 is more favorable (the formation of these species from **5a**, Ag_2CO_3 and PhI are exothermic by 10.1 and 16.3 kcal/mol, respectively) than their **5_3as** and **5_3ac** analogs with K_3PO_4 (the formation of which from **5a**, K_3PO_4 and PhI are exothermic only by 8.8 and 1.2 kcal/mol, respectively). We therefore also analyzed mechanism of the Ph–I bond activation and C-C coupling initiated from the complexes **5_3bs** and **5_3bc** with Ag_2CO_3. (see also Figure S8).

E. Additive (i.e. Ag_2CO_3) assisted ArI Activation. At first, we investigated the *nucleophilic substitution reaction* initiated from the intermediates **5_3bs** and **5_3bc**. We found that the reaction initiated by **5_3bs** proceeds with a 27.8 kcal/mol Ph–I activation free energy barrier at the transition state **TS3bs** (see Figure 6 and Figure S8), leads to the C–C coupled product, **5_4bs**, and is highly exergonic (by 69.7 kcal/mol). Since intermediate **5_3bs** is less favorable than its **5_3bc** isomer by 6.2 kcal/mol, the overall energy barrier, calculated from the lowest **5_3bc**, is 34.0 kcal/mol at the transition state **TS3bs** (see Figure 6). Whereas, the *nucleophilic substitution reaction*, initiated from the energetically most favorable isomer **5_3bc**, proceeds via the transition state **TS3bc** and

requires even larger, 38.9 kcal/mol, free energy barrier.

Thus, the above presented data for the reactive complexes with K_3PO_4 and Ag_2CO_3 show that the Ph–I bond activation and the following C–C coupling proceeding via the Cu-mediated nucleophilic substitution mechanism require high energy barrier for the Ph–I addition transition state.

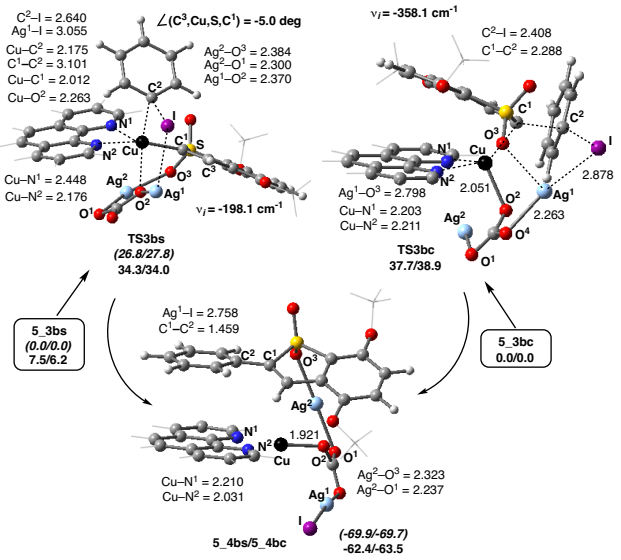

Figure 6. Transition states **TS3bs** and **TS3bc**, and product **5_4bs/5_4bc** of the Ar–I activation and C-C coupling initiated from **5_3bs** and **5_3bc**, along with their relative energies (calculated relative to complexes **5_3bc** and **5_3bs** *(in italic)*, respectively, in kcal/mol) and important geometry parameters (distances are in Å, but angles are in deg.).

The large energy barriers for the both base and additive assisted nucleophilic substitution reactions brought our attention to the idea of Ph–I oxidative addition to Ag^+ (Ag^1 in Figure 4). Here, we wish to mention that in recent years several Ag(I)/Ag(III) catalytic cycle for C-C and C-O cross-coupling reactions were reported and even some aryl-Ag(III) complexes were synthesized. [59]

***Silver-assisted oxidative addition*:** Gratifyingly, we found that the oxidative addition of Ph–I to Ag^+-center of **5_3bc** (which is energetically the most stable active intermediate with additive Ag_2CO_3) requires 24.2 kcal/mol activation barrier ($\Delta G^{\ddagger}$) at the transition state **TS3bc_ox.** This energy barrier is almost 9.8 kcal/mol smaller than that required for *Cu-mediated nucleophilic substitution*. As shown in Figure 7, in **TS3bc_ox**: (i) the activated Ph–I bond is elongated to 2.573 Å from 2.150 Å in **5_3bc**, (ii) the nascent Ag^1–C^2(Ar) and Ag^1–I bonds are 2.262 and 2.812 Å, respectively, and (iii) the Ag^1–C^1(DBT') and Ag^1–O^4 bond distance are only slightly changed. These geometrical features are consistent with the oxidative addition nature of **TS3bc_ox**. Consequently, the performed IRC calculations from the **TS3bc_ox** connected pre-reaction complex **5_3bc** and two-electron, Ag(I)/Ag(III), oxidation product **5_4bc_ox**. Overall the Ag(I)/Ag(III) oxidation process, i.e. reaction **5_3bc** → **TS3bc_ox** → **5_4bc_ox**, is calculated to be endergonic by 9.3 kcal/mol.

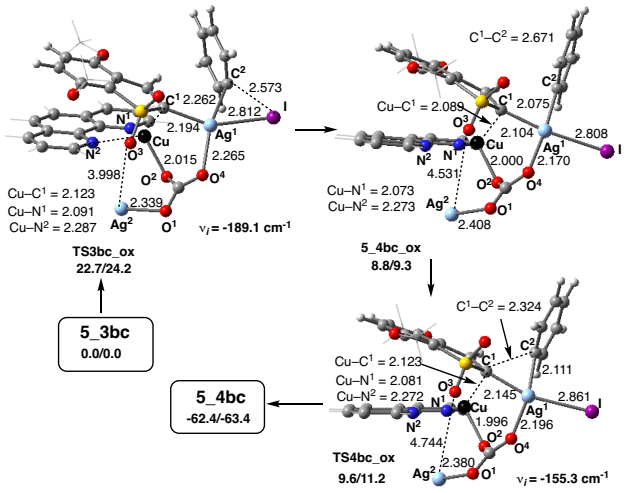

Figure 7. Transition states **TS3bc_ox**, **TS4bc_ox** and the Ag(III) oxidative addition intermediate **5_4bc_ox** of the Ar–I addition to Ag-center of **5_3bc** followed by the Ar-cation transfer to DBT' to form C-C bond. Relative energies (in kcal/mol) of these structures are calculated relative to the complex **5_3bc**. The presented important bond distances and angles of these structures are in Å and deg. respectively.

In the next step, the metastable Ag(III)-complex **5_4bc_ox** rearranges to the highly stable product complex **5_4bc**. The free energy barrier required for this transformation is only 1.9 kcal/mol through the transition state **TS4bc_ox**.

From the above results, it is clear that, in the absence of additive Ag_2CO_3, the DBT and PhI coupling is initiated from the complex **5_3as,** with base K_3PO_4, and proceeds via the *Cu-mediated nucleophilic substitution pathway with a* 34.5 kcal/mol rate-limiting Ph–I activation free energy barrier. In contrast, in the presence of the additive Ag_2CO_3, the DBT and PhI coupling start from the complex **5_3bc** and proceed via *the* Ph–I *oxidative addition to Ag(I)-center followed by reductive elimination,* which requires a 9.8 kcal/mol smaller (i.e. 24.2 kcal/mol) free energy barrier for Ph–I activation. Thus, the

presence of Ag_2CO_3 additive in the reaction mixture switches the mechanism of Ph–I activation and enhances the rate and yield of this reaction. This conclusion from computation is consistent with experiments showing that addition of Ag_2CO_3 in to the reaction mixture of (Phen)CuI, DBTT, Ar–I and K_3PO_4 increases the yield of the reaction.

Conclusion

Here, we have studied mechanisms of biaryl formation between DBT (model of DBTT) and aryl-iodide in the presence of CuI, phenanthroline (Phen), K_3PO_4 (as a base) and Ag_2CO_3 (as an additive). Briefly (see Scheme 4):

1. The first step of the reaction is the *I-to-base ligand exchange* in the pre-reaction complex (Phen)CuI, which occurs with a very small free energy barrier, and is highly exergonic

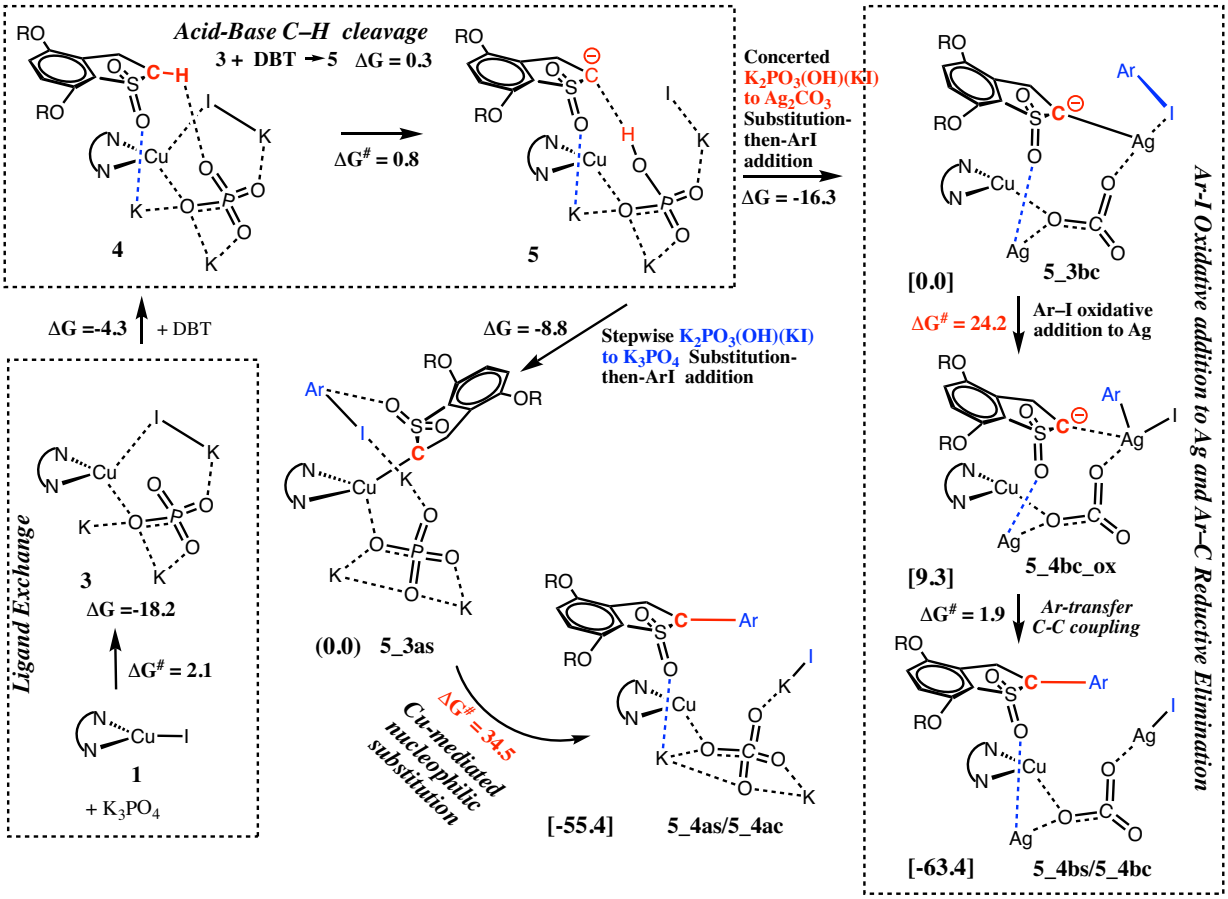

Scheme 4. Presentation of the predicted mechanism of the Ullmann-type biaryl formation between DBT and aryl-iodide in the presence of CuI (as a catalyst), phenanthroline (as a ligand), K_3PO_4 (as a base) and Ag_2CO_3 (as an additive).

2. The resulting intermediate coordinates substrate (DBT) and deprotonates the reactive C–H bond via an *acid-base mechanism*. It is shown that: (a) the presence of sulfonyl oxygens in DBT is essential. It interacts with the cation of the base to bring the substrate and base close to each other, and (b) the Cu-center of the catalyst plays an anchoring role. It is also shown that K_3PO_4 is a more effective base for deprotonation of DBT than Ag_2CO_3.

3. The resulting complex [(Phen)Cu][K_2PO_3(OH)(KI)](DBT'), transforms to [(Phen)Cu][K_3PO_4](DBT')(PhI), (**5_3as**), with a covalent Cu–C^1(DBT') bond, which is a direct analog of the previously reported[22] three-coordinated active (LL)Cu(Nu) intermediate for the Ullmann-type of coupling catalyzed by Cu(I) in the presence of the neutral and bidentate ancillary ligands (LL). The Ph–I activation and C–C coupling in **5_3as** *is a Cu-mediated nucleophilic substitution reaction*, and requires a significant free energy barrier (34.5 kcal/mol).

4. In contrast, in the presence of Ag_2CO_3, the intermediate [(Phen)Cu][K_2PO_3(OH)(KI)](DBT') transforms to [(Phen)Cu][Ag_2CO_3](DBT')(ArI),

(**5_3bc**), with an Ag–C[1](DBT') bond. In this complex, the Ph–I activation and C–C coupling proceed *via the oxidative addition of PhI on* Ag^{+} *followed by the reductive elimination.* This process requires 9.8 kcal/mol smaller (i.e. 24.2 kcal/mol) free energy barrier (see Scheme 4) than *Cu-mediated nucleophilic substitution.*

Thus, the presence of Ag_2CO_3 in the reaction mixture, as an additive, not only accelerates the DBT and PhI coupling, it also switches the mechanism of the reaction from the *Cu-mediated nucleophilic substitution* to the *Ag(I)-promoted oxidative addition-reductive elimination.*

ASSOCIATED CONTENT

Supporting Materials includes: (1) Interaction of complex **1** with K_3PO_4 and Ag_2CO_3, and ArI; (2) Catalyst activation by Ag_2CO_3 additive; (3) "The Ar–I activation first" pathway; Oxidative addition of ArI followed by deprotonation of the substrate by K_3PO_4; (4) "The Ar–I activation first" pathway; Oxidative addition of ArI followed by deprotonation of the substrate by Ag_2CO_3; (5) "The substrate C-H activation first" pathway by Ag_2CO_3; (6) Various mechanistic consideration of ArI activation; (7) Free energy surfaces of the base (i.e. K_3PO_4) assisted PhI Activation and C-C coupling; (8) Free energy surfaces of the additive (i.e. Ag_2CO_3) assisted PhI Activation and C-C coupling; (9) Catalyst regeneration; (10) Regioselectivity studies; (11) Cartesian coordinates and energy parameters. "This material is available free of charge *via* the Internet at http://pubs.acs.org."

AUTHOR INFORMATION

Corresponding Author

dmusaev@emory.edu, toby.nelson@okstate.edu

NOTES

The authors declare no competing financial interests.

ACKNOWLEDGMENT

This work was supported by the National Science Foundation under the CCI Center for Selective C–H Functionalization (CHE-1700982). We gratefully acknowledge NSF MRI-R2 grant (CHE-0958205 for D.G.M.) and the use of the resources of the Cherry Emerson Center for Scientific Computation, as well as Oklahoma State University Division of Institutional Diversity. Authors are thankful to Dr. Brandon Haines for help provided during the manuscript preparation.

REFERENCES

1. Bhuwalka, A.; Mike, J. F.; He, M.; Intemann, J. J.; Nelson, T.; Ewan, M. D.; Roggers, R. A.; Lin, Z.; Jeffries-El, M., Quaterthiophene–Benzobisazole Copolymers for Photovoltaic Cells: Effect of Heteroatom Placement and Substitution on the Optical and Electronic Properties. *Macromol.* **2011,** *44* (24), 9611-9617.
2. Ahmed, E.; Subramaniyan, S.; Kim, F. S.; Xin, H.; Jenekhe, S. A., Benzobisthiazole-Based Donor–Acceptor Copolymer Semiconductors for Photovoltaic Cells and Highly Stable Field-Effect Transistors. *Macromol.* **2011,** *44* (18), 7207-7219.
3. Zhou, J.; Zuo, Y.; Wan, X.; Long, G.; Zhang, Q.; Ni, W.; Liu, Y.; Li, Z.; He, G.; Li, C.; Kan, B.; Li, M.; Chen, Y., Solution-Processed and High-Performance Organic Solar Cells Using Small Molecules with a Benzodithiophene Unit. *J. Am. Chem. Soc.* **2013,** *135* (23), 8484-8487.
4. Chavez Iii, R.; Cai, M.; Tlach, B.; Wheeler, D. L.; Kaudal, R.; Tsyrenova, A.; Tomlinson, A. L.; Shinar, R.; Shinar, J.; Jeffries-El, M., Benzobisoxazole cruciforms: a tunable, cross-conjugated platform for the generation of deep blue OLED materials. *J. Mater. Chem. C* **2016,** *4* (17), 3765-3773.
5. Wang, P.; Verma, P.; Xia, G.; Shi, J.; Qiao, J. X.; Tao, S.; Cheng, P. T. W.; Poss, M. A.; Farmer, M. E.; Yeung, K. S.; Yu, J. Q., Ligand-accelerated non-directed C-H functionalization of arenes. *Nature* **2017,** *551* (7681), 489-493.
6. Lotz, M. D.; Camasso, N. M.; Canty, A. J.; Sanford, M. S., Role of silver salts in palladium-catalyzed arene and heteroarene C-H functionalization reactions. *Organometallics* **2017,** *36* (1), 165-171.
7. Jongbloed, L. S.; García-López, D.; Van Heck, R.; Siegler, M. A.; Carbó, J. J.; Van Der Vlugt, J. I., Arene C(sp2)-H Metalation at NiIIModeled with a Reactive PONC<inf>Ph</inf>Ligand. *Inorg. Chem.* **2016,** *55* (16), 8041-8047.
8. Larsen, M. A.; Hartwig, J. F., Iridium-catalyzed C-H borylation of heteroarenes: Scope, regioselectivity, application to late-stage functionalization, and mechanism. *J. Am. Chem. Soc.* **2014,** *136* (11), 4287-4299.
9. Rouquet, G.; Chatani, N., Catalytic functionalization of C(sp2)-H and C(sp3)-H bonds by

using bidentate directing groups. *Angew. Chem. Int. Ed.* **2013,** *52* (45), 11726-11743.
10. Murakami, K.; Yamada, S.; Kaneda, T.; Itami, K., C-H Functionalization of Azines. *Chem. Rev.* **2017,** *117* (13), 9302-9332.
11. Ley, S. V.; Thomas, A. W., Modern Synthetic Methods for Copper-Mediated C(aryl)□O, C(aryl)□N, and C(aryl)□S Bond Formation. *Angew. Chem. Int. Ed.* **2003,** *42* (44), 5400-5449.
12. Beletskaya, I. P.; Cheprakov, A. V., Copper in cross-coupling reactions: The post-Ullmann chemistry. *Coord. Chem. Rev.* **2004,** *248* (21-24), 2337-2364.
13. Monnier, F.; Taillefer, M., Catalytic C□C, C□N, and C□O Ullmann-Type Coupling Reactions: Copper Makes a Difference. *Angew. Chem. Int. Ed.* **2008,** *47* (17), 3096-3099.
14. Evano, G.; Blanchard, N.; Toumi, M., Copper-Mediated Coupling Reactions and Their Applications in Natural Products and Designed Biomolecules Synthesis. *Chem. Rev.* **2008,** *108* (8), 3054-3131.
15. Monnier, F.; Taillefer, M., Catalytic C□C, C□N, and C□O Ullmann-Type Coupling Reactions. *Angew. Chem. Int. Ed.* **2009,** *48* (38), 6954-6971.
16. Khambhati, D. P.; Sachinthani, K. A. N.; Rheingold, A. L.; Nelson, T. L., Regioselective copper-catalyzed direct arylation of benzodithiophene-S,S -tetraoxide. *Chem. Commun.* **2017,** *53* (37), 5107-5109.
17. Jones, G. O.; Liu, P.; Houk, K. N.; Buchwald, S. L., Computational explorations of mechanisms and ligand-directed selectivities of copper-catalyzed ullmann-type reactions. *J. Am. Chem. Soc.* **2010,** *132* (17), 6205-6213.
18. Yu, H. Z.; Jiang, Y. Y.; Fu, Y.; Liu, L., Alternative mechanistic explanation for ligand-dependent selectivities in copper-catalyzed N- and O-arylation reactions. *J. Am. Chem. Soc.* **2010,** *132* (51), 18078-18091.
19. Creutz, S. E.; Lotito, K. J.; Fu, G. C.; Peters, J. C., Photoinduced Ullmann C–N Coupling: Demonstrating the Viability of a Radical Pathway. *Science* **2012,** *338* (6107), 647-651.
20. Zhang, S.; Zhu, Z.; Ding, Y., Proposal for halogen atom transfer mechanism for Ullmann O-arylation of phenols with aryl halides. *Dalton Trans.* **2012,** *41* (45), 13832-13840.
21. Zhang, S. L.; Fan, H. J., Theoretical study on copper-catalyzed S -arylation of thiophenols with aryl halides: Evidence supporting the LCu(I)-SPh active catalyst and halogen atom transfer mechanism. *Organometallics* **2013,** *32* (17), 4944-4951.
22. Giri, R.; Brusoe, A.; Troshin, K.; Wang, J. Y.; Font, M.; Hartwig, J. F., Mechanism of the Ullmann Biaryl Ether Synthesis Catalyzed by Complexes of Anionic Ligands. Evidence for the Reaction of Iodoarenes With Ligated Anionic CuI Intermediates. *J. Am. Chem. Soc.* **2018**, *140*, 793-806.
23. Tao, C. Z.; Li, J.; Cui, X.; Fu, Y.; Guo, Q. X., Cu-catalyzed cross-couplings under ligandless conditions. *Chin. Chem. Lett.* **2007,** *18* (10), 1199-1202.
24. Kiyomori, A.; Marcoux, J. F.; Buchwald, S. L., An efficient copper-catalyzed coupling of aryl halides with imidazoles. *Tetrahedron Lett.* **1999,** *40* (14), 2657-2660.
25. Goodbrand, H. B.; Hu, N. X., Ligand-accelerated catalysis of the Ullmann condensation: Application to hole conducting triarylamines. *J. Org. Chem.* **1999,** *64* (2), 670-674.
26. Weng, Z.; He, W.; Chen, C.; Lee, R.; Tan, D.; Lai, Z.; Kong, D.; Yuan, Y.; Huang, K. W., An air-stable copper reagent for nucleophilic trifluoromethylthiolation of aryl halides. *Angew. Chem. Int. Ed.* **2013,** *52* (5), 1548-1552.
27. Zanon, J.; Klapars, A.; Buchwald, S. L., Copper-catalyzed domino halide exchange-cyanation of aryl bromides. *J. Am. Chem. Soc.* **2003,** *125* (10), 2890-2891.
28. Antilla, J. C.; Baskin, J. M.; Barder, T. E.; Buchwald, S. L., Copper-diamine-catalyzed N-arylation of pyrroles, pyrazoles, indazoles, imidazoles, and triazoles. *J. Org. Chem.* **2004,** *69* (17), 5578-5587.
29. Surry, D. S.; Buchwald, S. L., Diamine ligands in copper-catalyzed reactions. *Chem. Sci.* **2010,** *1* (1), 13-31.
30. Cristau, H. J.; Cellier, P. P.; Hamada, S.; Spindler, J. F.; Taillefer, M., A general and mild Ullmann-type synthesis of diaryl ethers. *Org. Lett.* **2004,** *6* (6), 913-916.
31. Ma, D.; Cai, Q., N,N-Dimethyl Glycine-Promoted Ullmann Coupling Reaction of Phenols and Aryl Halides. *Org. Lett.* **2003,** *5* (21), 3799-3802.
32. Fagan, P. J.; Hauptman, E.; Shapiro, R.; Casalnuovo, A., Using intelligent/random library screening to design focused libraries for the optimization of homogeneous catalysts: Ullmann ether formation. *J. Am. Chem. Soc.* **2000,** *122* (21), 5043-5051.
33. Buck, E.; Song, Z. J.; Tschaen, D.; Dormer, P. G.; Volante, R. P.; Reider, P. J., Ullmann Diaryl Ether Synthesis: Rate Acceleration by 2,2,6,6-Tetramethylheptane-3,5-dione. *Org. Lett.* **2002,** *4* (9), 1623-1626.

34. De Lange, B.; Lambers-Verstappen, M. H.; Schmieder-Van De Vondervoort, L.; Sereinig, N.; De Rijk, R.; De Vries, A. H. M.; De Vries, J. G., Aromatic amination of aryl bromides catalysed by copper/β-diketone catalysts: The effect of concentration. *Synlett* **2006,** (18), 3105-3109.
35. Wang, D.; Cai, Q.; Ding, K., An efficient copper-catalyzed amination of aryl halides by aqueous ammonia. *Adv. Synth. Catal.* **2009,** *351* (11-12), 1722-1726.
36. Tye, J. W.; Weng, Z.; Johns, A. M.; Incarvito, C. D.; Hartwig, J. F., Copper complexes of anionic nitrogen ligands in the amidation and imidation of aryl halides. *J. Am. Chem. Soc.* **2008,** *130* (30), 9971-9983.
37. Strieter, E. R.; Bhayana, B.; Buchwald, S. L., Mechanistic studies on the copper-catalyzed N-arylation of amides. *J. Am. Chem. Soc.* **2009,** *131* (1), 78-88.
38. Giri, R.; Hartwig, J. F., Cu(I)-amido complexes in the ullmann reaction: Reactions of Cu(I)-amido complexes with iodoarenes with and without autocatalysis by CuI. *J. Am. Chem. Soc.* **2010,** *132* (45), 15860-15863.
39. Tye, J. W.; Weng, Z.; Giri, R.; Hartwig, J. F., Copper(I) Phenoxide complexes in the etherification of aryl halides. *Angew. Chem. Int. Ed.* **2010,** *49* (12), 2185-2189.
40. Huang, Z.; Hartwig, J. F., Copper(I) enolate complexes in α-arylation reactions: Synthesis, reactivity, and mechanism. *Angew. Chem. Int. Ed.* **2012,** *51* (4), 1028-1032.
41. Sambiagio, C.; Marsden, S. P.; Blacker, A. J.; McGowan, P. C., Copper catalysed Ullmann type chemistry: From mechanistic aspects to modern development. *Chem. Soc. Rev.* **2014,** *43* (10), 3525-3550.
42. Rovira, M.; Jašíková, L.; Andris, E.; Acuña-Parés, F.; Soler, M.; Güell, I.; Wang, M. Z.; Gómez, L.; Luis, J. M.; Roithová, J.; Ribas, X., A CuI/CuIIIprototypical organometallic mechanism for the deactivation of an active pincer-like CuIcatalyst in Ullmann-type couplings. *Chem. Commun.* **2017,** *53* (62), 8786-8789.
43. Rovira, M.; Soler, M.; Güell, I.; Wang, M. Z.; Gómez, L.; Ribas, X., Orthogonal Discrimination among Functional Groups in Ullmann-Type C-O and C-N Couplings. *J. Org. Chem.* **2016,** *81* (17), 7315-7325.
44. Soria-Castro, S. M.; Andrada, D. M.; Caminos, D. A.; Argüello, J. E.; Robert, M.; Peñéñory, A. B., Mechanistic Insight into the Cu-Catalyzed C-S Cross-Coupling of Thioacetate with Aryl Halides: A Joint Experimental-Computational Study. *J. Org. Chem.* **2017,** *82* (21), 11464-11473.
45. Job, G. E.; Buchwald, S. L., Copper-catalyzed arylation of β-amino alcohols. *Org. Lett.* **2002,** *4* (21), 3703-3706.
46. Klapars, A.; Huang, X.; Buchwald, S. L., A general and efficient copper catalyst for the amidation of aryl halides. *J. Am. Chem. Soc.* **2002,** *124* (25), 7421-7428.
47. Mondal, J.; Biswas, A.; Chiba, S.; Zhao, Y., Cu0 Nanoparticles Deposited on Nanoporous Polymers: A Recyclable Heterogeneous Nanocatalyst for Ullmann Coupling of Aryl Halides with Amines in Water. *Sci. Rep.* **2015,** *5*, 8294.
48. Gurjar, K. K.; Sharma, R. K., Mechanistic Studies of Ullmann-Type C-N Coupling Reactions: Carbonate-Ligated Copper(III) Intermediates. *Chemcatchem* **2017,** *9* (5), 862-869.
49. Frisch, M. J.; Trucks, G. W.; Schlegel, H. B.; Scuseria, G. E.; Robb, M. A.; Cheeseman, J. R.; Scalmani, G.; Barone, V.; Mennucci, B.; Petersson, G. A.; Nakatsuji, H.; Caricato, M.; Li, X.; Hratchian, H. P.; Izmaylov, A. F.; Bloino, J.; Zheng, G.; Sonnenberg, J. L.; Hada, M.; Ehara, M.; Toyota, K.; Fukuda, R.; Hasegawa, J.; Ishida, T.; Nakajima, M.; Honda, Y.; Kitao, O.; Nakai, H.; Vreven, T.; Montgomery, J., J. A. ; Peralta, J. E.; Ogliaro, F.; Bearpark, M.; Heyd, J. J.; Brothers, E.; Kudin, K. N.; Staroverov, V. N.; Keith, T.; Kobayashi, R.; Normand, J.; Raghavachari, K.; Rendell, A.; Burant, J. C.; Iyengar, S. S.; Tomasi, J.; Cossi, M.; Rega, N.; Millam, J. M.; Klene, M.; Knox, J. E.; Cross, J. B.; Bakken, V.; Adamo, C.; Jaramillo, J.; Gomperts, R.; Stratmann, R. E.; Yazyev, O.; Austin, A. J.; Cammi, R.; Pomelli, C.; Ochterski, J. W.; Martin, R. L.; Morokuma, K.; Zakrzewski, V. G.; Voth, G. A.; Salvador, P.; Dannenberg, J. J.; Dapprich, S.; Daniels, A. D.; Farkas, O.; Foresman, J. B.; Ortiz, J. V.; Cioslowski, J.; Fox, D. J. *Gaussian 09, Revision E.01*, Gaussian, Inc., Wallingford CT, 2013.
50. Lee, C.; Yang, W.; Parr, R. G., Development of the Colle-Salvetti correlation-energy formula into a functional of the electron density. *Phy. Rev. B* **1988,** *37* (2), 785-789.
51. Becke, A. D., Density-functional thermochemistry. III. The role of exact exchange. *J. Chem. Phy.* **1993,** *98* (7), 5648-5652.
52. Hay, P. J.; Wadt, W. R., Ab initio effective core potentials for molecular calculations. Potentials for the transition metal atoms Sc to Hg. *J. Chem. Phy.* **1985,** *82* (1), 270-283.
53. Hay, P. J.; Wadt, W. R., Ab initio effective core potentials for molecular calculations. Potentials for K to Au including the outermost core orbitale. *J. Chem. Phy.* **1985,** *82* (1), 299-310.
54. Grimme, S.; Antony, J.; Ehrlich, S.; Krieg, H., A consistent and accurate ab initio

parametrization of density functional dispersion correction (DFT-D) for the 94 elements H-Pu. *J. Chem. Phy.* **2010,** *132* (15), 154104(1-19).
55. Barone, V.; Cossi, M.; Tomasi, J., A new definition of cavities for the computation of solvation free energies by the polarizable continuum model. *J. Chem. Phy.* **1997,** *107* (8), 3210-3221.
56. Tomasi, J.; Mennucci, B.; Cancès, E., The IEF version of the PCM solvation method: An overview of a new method addressed to study molecular solutes at the QM ab initio level. *J. Mol. Struct. (Theochem.)* **1999,** *464* (1-3), 211-226.
57. Böes, E. S.; Livotto, P. R.; Stassen, H., Solvation of monovalent anions in acetonitrile and N,N-dimethylformamide: Parameterization of the IEF-PCM model. *Chem. Phy.* **2006,** *331* (1), 142-158.
58. Choudary, B. M.; Sridhar, C.; Kantam, M. L.; Venkanna, G. T.; Sreedhar, B., Design and evolution of copper apatite catalysts for N-arylation of heterocycles with chloro- and fluoroarenes. *J. Am. Chem. Soc.* **2005,** *127* (28), 9948-9949.
59. Font, M.; Acuña-Parés, F.; Parella, T.; Serra, J.; Luis, J. M.; Lloret-Fillol, J.; Costas, M.; Ribas, X., Direct observation of two-electron Ag(I)/Ag(III) redox cycles in coupling catalysis. *Nat. Commun.* **2014,** *5*.

Unveiling the Role of Base and Additive in the Ullmann-type of Arene-Aryl C-C Coupling Reaction

Ajitha J. Manjaly,[a] Fathima Pary,[b] Toby L. Nelson[b,*], and Djamaladdin G. Musaev[a,*]

[a] Cherry L. Emerson Center for Scientific Computation, and Department of Chemistry, Emory University, 1515 Dickey Drive, Atlanta, Georgia 30322

[b] Department of Chemistry, Oklahoma State University, 107 Physical Science, Stillwater, Oklahoma 74078